



## RAPID COMMUNICATION

# A novel mouse model of PEDF-associated serious liver inflammation, hepatic tumorigenesis and cardiovascular injury mimics human nonalcoholic steatohepatitis



There are no approved therapeutic drugs for nonalcoholic steatohepatitis (NASH) due to the many bottlenecks, including the lack of preclinical animal models that can perfectly mimic human NASH features, such as systemic metabolic disorders, hepatic steatosis, intense liver inflammation and fibrosis, liver tumorigenesis, and cardiovascular complications.<sup>1,2</sup> Pigment epithelium-derived factor (PEDF) is a lipid metabolism regulator with high expression in the liver, and its reduced expression in the liver is closely related to the development of nonalcoholic fatty liver disease (NAFLD).<sup>3,4</sup> Besides, high-fat diet (HFD)-fed low-density lipoprotein receptor knockout (LDLR knockout, LKO) mice are often used as animal models to study atherosclerosis and fatty liver.<sup>5</sup> Here, we attempt to further knock out PEDF in HFD-fed LKO mice to induce premature development of inflammation and fibrosis, leading to a better NASH model. The results showed that HFD-fed LDLR/PEDF double knockout (LDLR/PEDF DKO, L/P DKO) mice can ideally mimic the disease progression and pathological characteristics of human NASH, not only show systemic changes but also experience disease progression from mild to severe NASH accompanied by serious liver inflammation, tumorigenesis, and cardiovascular injury. The multiomics analysis and related validation results suggest that PEDF deficiency is involved in the occurrence and development of NASH by affecting lipid and glutathione metabolism.

Animals of the wild-type (WT) + standard chow diet (SCD), WT + HFD, LKO + HFD, and L/P DKO + HFD groups were sampled and tested at 32 and 48 weeks after the start of the experiment. The body weight (BW), circulating total cholesterol (TC), and triglycerides (TG) levels in L/P DKO

mice were significantly increased compared to those in other groups of animals after HFD feeding for 32 and/or 48 weeks (Fig. S1A–C). Furthermore, the results of the intra-peritoneal glucose tolerance test (IPGTT) and the intra-peritoneal insulin tolerance test (IPITT) confirmed that L/P DKO mice exhibited significantly impaired insulin and glucose tolerance compared to other groups of animals after HFD feeding for 32 weeks (Fig. S1D, E). Moreover, the serum insulin (INS) and blood glucose levels in L/P DKO mice were significantly increased compared to those in other groups of animals after HFD feeding for 32 and 48 weeks (Fig. S1F, G).

We then evaluated the liver lesions in each group of animals by biochemical and pathological indices. After 32 weeks of HFD feeding, L/P DKO mice exhibited a more severe fatty liver phenotype than animals in other groups, as evidenced mainly by a significantly larger liver size, higher liver weight (LW), LW/BW ratio, and serum glutamic pyruvic transaminase (ALT) and glutamic oxaloacetic transaminase (AST) levels, and more severe hepatic steatosis and ballooning degeneration than animals in the other groups (Fig. S2A–H). However, although the L/P DKO mice at this time point had significantly higher levels of liver inflammation and fibrosis than animals in the WT + SCD and WT + HFD groups, they were not significantly different from animals in the LKO + HFD group and still exhibited a mild NASH phenotype (Fig. S2I–K). In contrast, after 48 weeks of HFD feeding, L/P DKO mice not only exhibited a significantly higher LW, LW/BW ratio, and serum ALT and AST levels than the other groups of animals but also a significant difference in the change from hepatic steatosis and ballooning degeneration to hepatic inflammation and

Peer review under responsibility of Chongqing Medical University.

<https://doi.org/10.1016/j.gendis.2023.01.011>

2352-3042/© 2023 The Authors. Publishing services by Elsevier B.V. on behalf of KeAi Communications Co., Ltd. This is an open access article under the CC BY-NC-ND license (<http://creativecommons.org/licenses/by-nc-nd/4.0/>).

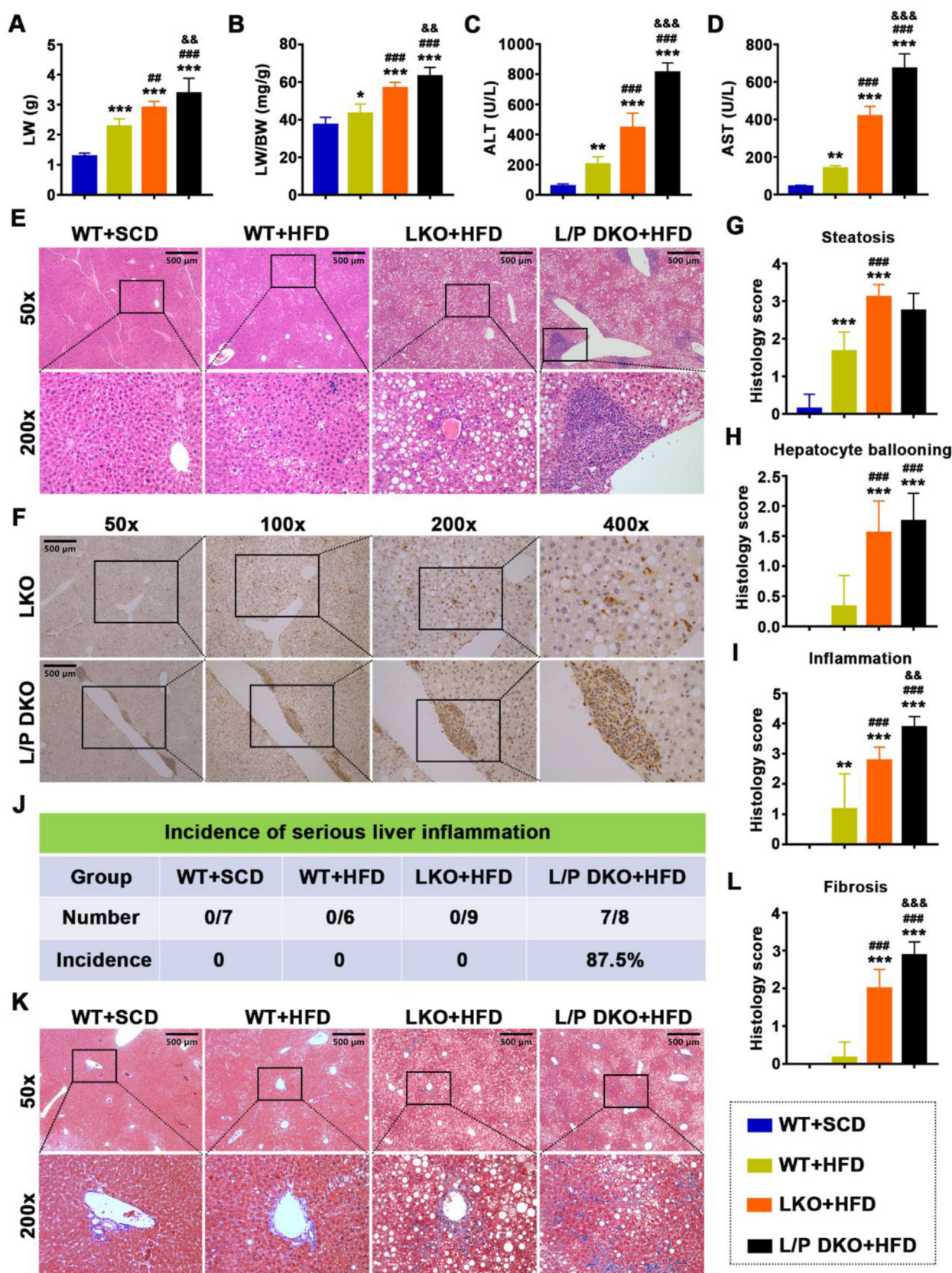


**Figure 1** L/P DKO mice develop hepatic steatosis, ballooning degeneration, serious liver inflammation, and severe fibrosis (HFD for 48 weeks). (A) LW ( $n = 6-9$ ). (B) LW/BW ratio ( $n = 6-9$ ). (C) Serum ALT levels ( $n = 6$ ). (D) Serum AST levels ( $n = 6$ ). (E) Liver HE staining ( $50\times$ ,  $200\times$ ) and (F) CD45 immunohistochemistry staining ( $200\times$ ) of representative mice in the groups of WT + SCD, WT + HFD, LKO + HFD, and L/P DKO + HFD. Histology score for steatosis (G), hepatocyte ballooning (H), and lobular inflammation

fibrosis compared with LKO mice. Thus, they exhibited a serious NASH phenotype accompanied by serious hepatic inflammation and severe hepatic fibrosis, as shown by HE staining and leukocyte common antigen (CD45) immunohistochemistry staining (Fig. 1A–L).

We further observed liver tumorigenesis in each group of animals by means of imaging and pathology. The results showed that no hepatic tumors developed in WT or LKO mice after 48 weeks of HFD or SCD feeding; however, some (3 of 8) L/P DKO mice fed an HFD developed hepatic tumors. These tumors were characterized mainly by liver nodules with high glucose uptake, as revealed by PET/CT, neoplastic lesions of hepatocellular adenoma with nodules and local abnormal hyperplasia within the nodules, and high expression of alpha-fetoprotein (AFP), as revealed by gross observation and pathological and immunohistochemical analyses (Fig. S3A–E). Additionally, immunohistochemical staining for proliferating cell nuclear antigen (PCNA) and platelet endothelial cell adhesion molecule 1 (CD31) confirmed the presence of substantial hepatocyte proliferation and vascular hyperplasia in the tumor area in HFD-fed L/P DKO mice but not in any other group of animals (Fig. S3F, G).

Further, imaging and pathological methods were used to observe cardiovascular injury in each group of animals. The vascular ultrasound results showed that the end-diastolic Ao Diam, the end-systolic Ao diam, and the AV Peak Vel were significantly higher in the L/P DKO mice than mice of WT + SCD and WT + HFD and (or not and) LKO + HFD groups at 32 and/or 48 weeks of HFD induction, while the Desc Ao Vel was not changed (Fig. S4A–G, 5A–G). The results of whole aortic oil red O staining showed that the proportion of aortic plaque area in L/P DKO mice was significantly increased compared to that in the other groups of animals (Fig. S5H, I). More importantly, after 48 weeks of HFD induction, the results of HE staining of myocardial tissue sections showed that L/P DKO mice exhibited significant cardiomyocyte hypertrophy, while the other groups of animals had no myocardial hypertrophy (Fig. S5J, K). These data suggest that L/P DKO mice develop a severe cardiovascular injury.

Finally, the lipidomics data showed that a total of 157 differential lipid molecules from different categories of lipids were identified including 107 glycerophospholipid (GP), 33 glycerolipids (GL), and 13 sphingolipid (SP) components and others (Fig. S6A–C). Further analysis showed that PEDF deficiency significantly exacerbated the disorder of hepatic GP, SP, and GL metabolism in LKO mice, mainly featured by consistent down-regulation of phosphatidylglycerol (PG) and lysophosphatidylglycerol (LPG) components, consistent up-regulation of sphingomyelin (SM) components, as well as consistent or inconsistent alterations in the content of diglyceride (DG) and TG

components (Fig. S6D–G). Besides, a total of 432 differentially expressed genes (DEGs) were identified by transcriptomics (Fig. S7A). Kyoto Encyclopedia of Genes and Genomes (KEGG) results showed that the glutathione (GSH) metabolism pathway was more significantly enriched in addition to the pathways related to lipid metabolism (Fig. S7B). Additionally, Gene Ontology (GO) and Gene Set Enrichment Analysis (GSEA) results also further suggest that PEDF deficiency leads to the inhibition of GSH metabolism (Fig. S7C, D). The protein–protein interaction (PPI) network analysis results of the top 50 hub genes showed that a large number of genes related to GSH metabolism are involved in the network of PEDF action (Fig. S7E). The further validation results showed that the GSH content in the liver of HFD-fed L/P DKO mice were significantly decreased compared to HFD-fed LKO mice (Fig. S7F–C). Taking into account the effect of GSH metabolism on lipid peroxidation and DNA damage, we tested the expression of lipid peroxidation marker 4-hydroxynonenal (4-HNE) and DNA damage marker 8-hydroxy-2 deoxyguanosine (8-OHdG) in the liver of each group of animals. The results showed that the expression of 4-HNE and the number of 8-OHdG positive cells per 400 × field in the liver of HFD-fed L/P DKO mice were significantly increased compared to HFD-fed LKO mice (Fig. S7G, H).

In summary, this study provides a novel NASH mouse model with serious liver inflammation, tumorigenesis, and cardiovascular injury that can be used as tools to enable the preclinical evaluation of drugs for NASH.

## Ethics declaration

All studies involving animal experimentation were approved by the Animal Care and Ethics Committee of Sun Yat-sen University.

## Author contributions

W. Cai and X. Li designed the project, researched the data, and wrote the manuscript. X. Li, H. Wang, Y. Wu, L. Zou, S. Deng, and X. Fu performed the experiments and analyzed the data. T. Huang, C. Shen, and T. Wu contributed to the discussion and provided helpful suggestions. W. Cai is the guarantor of this work and, as such, has full access to all the data in the study and takes responsibility for the integrity of the data and the accuracy of the data analysis.

## Funding

This research was funded by the National Key Research and Development Program of China (No. 2019YFA0801403), the

(I) based on HE staining (200 × ) ( $n = 5$ ). (J) Incidence of serious liver inflammation in each group of mice. (K) Liver Masson's Trichrome staining (50 × , 200 × ) of representative mice in the groups of WT + SCD, WT + HFD, LKO + HFD, and L/P DKO + HFD. Histology score for fibrosis (L) based on Masson's Trichrome staining (200 × ) ( $n = 5$ ). The data were expressed as the mean ± standard deviation. \* $P < 0.05$  vs. WT + SCD group, \*\* $P < 0.01$  vs. WT + SCD group, \*\*\* $P < 0.001$  vs. WT + SCD group, <sup>##</sup> $P < 0.01$  vs. WT + HFD group, <sup>###</sup> $P < 0.001$  vs. WT + HFD group, <sup>&&</sup> $P < 0.01$  vs. LKO + HFD group, <sup>&&&</sup> $P < 0.001$  vs. LKO + HFD group.

National Natural Science Foundation of China (No. 81670256, 81970219, 82170261, 82000250, 81741117), Guangdong Basic and Applied Basic Research Foundation (China) (No. 2021A1515011005, 2021B1212040006), China Postdoctoral Science Foundation (No. 2020M672976) and the Fundamental Research Funds for the Central University, Sun Yat-sen University, China (No. 22qntd4808). The funders had no role in the study design, data collection, analysis, decision to publish, or preparation of the manuscript.

## Conflict of interests

The authors declare that no competing interests exist.

## Appendix A. Supplementary data

Supplementary data to this article can be found online at <https://doi.org/10.1016/j.gendis.2023.01.011>.

## References

1. Asgharpour A, Cazanave SC, Pacana T, et al. A diet-induced animal model of non-alcoholic fatty liver disease and hepatocellular cancer. *J Hepatol.* 2016;65(3):579–588.
2. Tsuchida T, Lee YA, Fujiwara N, et al. A simple diet- and chemical-induced murine NASH model with rapid progression of steatohepatitis, fibrosis and liver cancer. *J Hepatol.* 2018;69(2):385–395.
3. Huang KT, Chen KD, Hsu LW, et al. Decreased PEDF promotes hepatic fatty acid uptake and lipid droplet formation in the pathogenesis of NAFLD. *Nutrients.* 2020;12(1):270.
4. Niyogi S, Ghosh M, Adak M, et al. PEDF promotes nuclear degradation of ATGL through COP1. *Biochem Biophys Res Commun.* 2019;512(4):806–811.
5. Véniant MM, Withycombe S, Young SG. Lipoprotein size and atherosclerosis susceptibility in Apoe (-/-) and Ldlr (-/-) mice. *Arterioscler Thromb Vasc Biol.* 2001;21(10):1567–1570.

Xinghui Li<sup>a,b,\*\*,1</sup>, Haiping Wang<sup>a,b,1</sup>, Yandi Wu<sup>a,b,1</sup>,  
Li Zou<sup>c</sup>, Shijie Deng<sup>a,b</sup>, Xinlu Fu<sup>a,b</sup>,  
Tongsheng Huang<sup>a,b</sup>, Conghui Shen<sup>a,b</sup>, Teng Wu<sup>a,b</sup>,  
Weibin Cai<sup>a,b,d,\*</sup>

<sup>a</sup> Guangdong Engineering & Technology Research Center for Disease-Model Animals, Laboratory Animal Center, Zhongshan School of Medicine, Sun Yat-sen University, Guangzhou, Guangdong 510080, China

<sup>b</sup> Department of Biochemistry, Zhongshan School of Medicine, Sun Yat-sen University, Guangzhou, Guangdong 510080, China

<sup>c</sup> School of Pharmacy, Guangdong Pharmaceutical University, Guangzhou, Guangdong 510006, China

<sup>d</sup> Guangdong Provincial Key Laboratory of Digestive Cancer Research, The Seventh Affiliated Hospital of Sun Yat-sen University, Shenzhen, Guangdong 518107, China

\*Corresponding author. 74 Zhongshan Road II, Guangzhou, Guangdong 510080, China.

\*\*Corresponding author. Guangdong Engineering & Technology Research Center for Disease-Model Animals, Laboratory Animal Center, Zhongshan School of Medicine, Sun Yat-sen University, Guangzhou, Guangdong 510080, China.  
E-mail addresses: [lixingh9@mail.sysu.edu.cn](mailto:lixingh9@mail.sysu.edu.cn) (X. Li),  
[caiwb@mail.sysu.edu.cn](mailto:caiwb@mail.sysu.edu.cn) (W. Cai)

28 October 2022

Available online 23 March 2023

<sup>1</sup> These authors contributed equally to this work and are joint first authors.